Nuclear Instruments and Methods in Physics Research A 742 (2014) 29–34

Contents lists available at ScienceDirect

Nuclear Instruments and Methods in Physics Research A

journal homepage: www.elsevier.com/locate/nima

Latest results from the telescope array

Peter Tinyakov

Service de Physique Théorique CP225, Université Libre de Bruxelles, Blvd du Triomphe, 1050 Bruxelles, Belgium

for the Telescope Array Collaboration

ARTICLE INFO

Available online 14 November 2013

Keywords:
Ultra-high energy cosmic rays
Spectrum
Mass composition
Anisotropy

ABSTRACT

The Telescope Array ultra-high energy cosmic ray detector, situated in Utah, USA, is taking data since March 2008. We will present the latest results of the spectrum, composition and anisotropy studies based on the 4 years of the Telescope Array data.

1. The telescope array experiment

The Telescope Array (TA) detector is a hybrid detector of ultra-high energy cosmic rays located in the Northern hemisphere in Utah, USA (39°17′48″N, 112°54′31″W). It consists of the surface detector (SD) composed of 507 scintillator detectors covering the area of approximately 700 km^2 (for details see [1]). The atmosphere over the surface array is viewed by 38 fluorescence telescopes arranged in 3 stations [2], which constitute the fluorescence detector (FD) of TA.

The TA detector is fully operational starting from March 2008. In this paper we will present the results based on the analysis of the first 4 years of TA data. An update is expected soon that will include the full first 5 year of data.

The scientific goals of TA include determination of the energy spectrum of UHECR, their mass composition, and investigation of anisotropies of UHECR in the Northern sky. The ultimate purpose is to unveil the nature and origin of UHECR.

2. Data

Different subsets of the TA data are optimized for different studies. For the measurement of the spectrum of UHECR, the high quality surface detector (SD) events have been selected by the following criteria: the zenith angle $<45^\circ$, shower core must be inside the array at a more than 1200 m from the border, number of detectors hit is 5 or larger, the quality of the reconstruction fit is $\chi^2/\text{d.o.f} < 4$, pointing direction resolution is better than 5°, the fractional uncertainty of the energy estimator $S(800)$ is less than 0.25. In the 4-year period from May 2008 until May 2012, there are 13,100 events above $10^{18.2}$ eV satisfying these criteria. The aperture of TA SD with the above cuts is 920 km^2 sr, while the total exposure corresponding to this set is 3690 km^2 sr yr. Further details can be found in Ref. [3].

A different data set has been compiled for anisotropy studies. The idea here is to loosen the cuts in order to increase statistics, without decreasing significantly the data quality. This may be achieved by extending the zenith angle cut to $<55^\circ$ and relaxing the border cut. This anisotropy set contains 1807 events with energies $E > 10$ EeV, 114 events with $E > 40$ EeV, and 42 events with $E > 57$ EeV.

By comparing the thrown and reconstructed arrival directions of the simulated data sets, the angular resolution of TA events with $E > 10$ EeV was found to be approximately 1.5°. Events with zenith angles between 45° and 55° have even better angular resolution. The energy resolution of the TA surface detector at $E > 10$ EeV is close to 20% [3].

In the anisotropy studies the crucial role is played by the exposure function. The exposure of the TA SD detector was calculated by the Monte-Carlo technique with the full simulation of the detector. It follows from these Monte-Carlo simulations that above 10 EeV the efficiency of the TA SD is 100%, while the exposure is indistinguishable from the geometrical one.

For the mass composition studies the stereo FD data have been used. These will be described in the corresponding section below.

3. The energy spectrum

The energy spectrum of UHECR is reconstructed from the SD data. The density of shower particles at a lateral distance of 800 m from the core, $S(800)$, is used as the energy estimator. This quantity is obtained by a lateral distribution fit, with the same functional form as used by the AGASA experiment. The energy is then estimated by using a look-up table in $S(800)$ and the zenith angle determined from an exhaustive MC simulation.

0168-9002/$ - see front matter © 2013 Elsevier B.V. All rights reserved.
http://dx.doi.org/10.1016/j.nima.2013.10.067

The absolute energy scale derived from the SD data alone is prone to large systematic uncertainties and possible biases associated with the modeling of hadronic interactions. On the other hand, the energy scale uncertainty is experimentally well-controlled for the FD events. We therefore correct our energy scale to the TA FD using events seen in common between the FD and SD. The observed differences between the FD and SD events are well described by a simple proportionality relationship, the SD energy scale being 27% higher than the FD. This correction is included in the spectrum shown below.

Fig. 1 shows the spectrum measured by the TA SD, where the differential flux multiplied by e^3 is shown. One can see the ankle structure and the suppression at the highest energies. A fit to a broken power law determines the energies of these features. The fit finds the ankle at an energy of $(4.6 \pm 0.3) \times 10^{18}$ eV and the suppression at $(5.4 \pm 0.6) \times 10^{19}$ eV. The power exponents for the three regions (below the ankle, between the breaks, and above the suppression) are 3.34 ± 0.04, 2.67 ± 0.03, and 4.6 ± 0.6, respectively. Also shown in Fig. 1 are the spectra reported by other experiments as indicated on the plot. The HiRes and TA SD spectra agree very well, both in the energy region above $10^{18.85}$ eV where the TA SD is 100% efficient, and also at lower energies where TA employs a substantial efficiency correction.

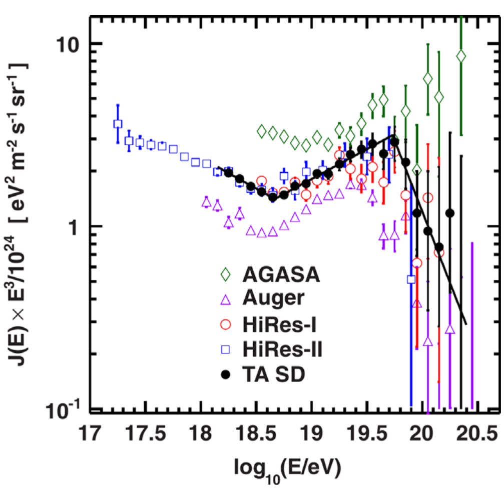

Fig. 1. TA SD energy spectrum (black points). The black lines show fit to a broken power law as described in the text. Also shown are measurements by other experiments as indicated on the plot.

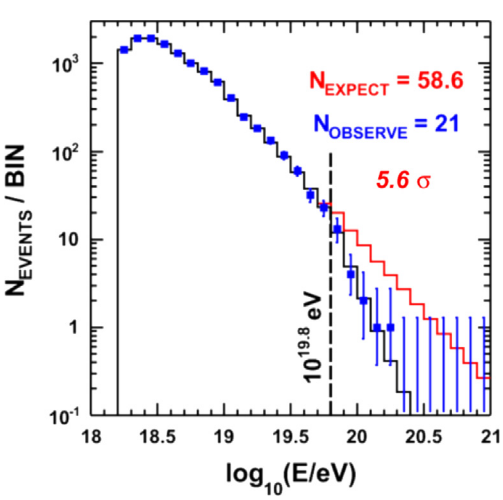

Fig. 2. Calculation of the significance of the break in the spectrum.

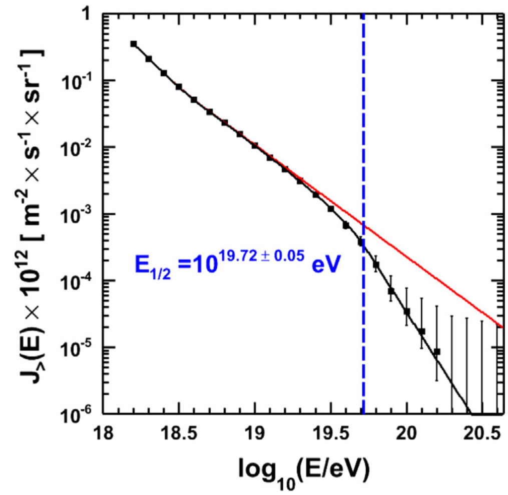

Fig. 3. $E_{1/2}$ is the energy at which the integral spectrum falls to one-half of its expected value in the absence of the cutoff.

The significance of the cutoff may be inferred by a linear extrapolation of the power law beyond the suppression point, see Fig. 2. The extrapolation predicts 58.6 events above the break, whereas TA observed only 21 events. This difference corresponds to a Poisson probability of 1.44×10^{-8}, or 5.6 standard deviations significance.

A related observable is $E_{1/2}$, the energy at which the integral spectrum falls to one-half of its expected value in the absence of the GZK cutoff (Fig. 3). This value is predicted to be $10^{19.72}$ eV for protons [4]. TA measures $\log_{10} E_{1/2} = 19.72 \pm 0.05$. Thus, the energy of the cutoff is consistent with the interpretation that the composition is protonic.

4. Mass composition

The observable sensitive to the nature of primary particle is the shower depth X_{max}, the atmospheric depth of the maximum of the shower. This quantity can only be directly measured by the fluorescent detector, so the FD data have to be used in the composition analysis. TA stereo data is used in the present analysis. Because of the large fluctuations, the composition can only be inferred from statistical quantities such as the mean value and RMS of X_{max}.

The expected distribution of X_{max} was estimated by the MC shower simulation code CORSIKA. The shower library was generated using a primary energy between 10^{18} eV and 10^{20} eV. Primary particle type was taken to be protons or iron nuclei. QGSJET-I, QGSJET-II and SYBILL were used for the hadronic interaction models. The generated showers were then run through the reconstruction procedure (including the full simulation of the detector) identical to that used for the real data, in order to determine the expected X_{max} distribution that includes all reconstruction and selection biases. In this way, the expectations for proton and iron primaries are obtained that can be compared to the real data.

Fig. 4 shows the comparison between the measured X_{max} and that expected for proton (red lines) and iron (blue lines) in several models as indicated on the plot. The TA data are better compatible with proton composition at all, including highest energies.

In Fig. 5 we show the comparison of the observed X_{max} distributions to those expected for proton and iron bin-by-bin in energy. Black points represent the data. Red (blue) histograms show MC simulations for protons (iron). As one can see, the